Structure of the Eukaryotic Initiation Factor (eIF) 5 Reveals a Fold Common to Several Translation Factors[†,‡]

Maria R. Conte,[*,§,⊗,||] Geoff Kelly,[⊥] Jeff Babon,[¶] Domenico Sanfelice,[§,⊗,||] James Youell,[§,⊗,||] Stephen J. Smerdon,[#] and Christopher G. Proud[£,∞,▽]

Biophysics Laboratories, School of Biological Sciences, University of Portsmouth, Portsmouth PO1 2DT, United Kingdom, Randall Division of Cell and Molecular Biophysics, King's College London, Guy's Campus, London SE1 1UL, United Kingdom, Biomedical NMR Centre and Division of Protein Structure, National Institute for Medical Research, The Ridgeway, Mill Hill, London NW7 1AA, United Kingdom, The Walter and Eliza Hall Institute of Medical Research, 1G Royal Parade, Parkville, Victoria 3050, Australia, Division of Molecular Physiology, School of Life Sciences, University of Dundee, Dundee, DD1 5EH, United Kingdom, and Department of Biochemistry and Molecular Biology, University of British Columbia, Life Science Centre, 2350 Health Science Mall, Vancouver, V6T 1Z3, Canada

Received November 22, 2005; Revised Manuscript Received February 16, 2006

ABSTRACT: Eukaryotic initiation factor 5 (eIF5) plays multiple roles in translation initiation. Its N-terminal domain functions as a GTPase-activator protein (GAP) for GTP bound to eIF2, while its C-terminal region nucleates the interactions between multiple translation factors, including eIF1, which acts to inhibit GTP hydrolysis or P_i release, and the β subunit of eIF2. These proteins and the events in which they participate are critical for the accurate recognition of the correct start codon during translation initiation. Here, we report the three-dimensional solution structure of the N-terminal domain of human eIF5, comprising two subdomains, both reminiscent of nucleic-acid-binding modules. The N-terminal subdomain contains the "arginine finger" motif that is essential for GAP function but which, unusually, resides in a partially disordered region of the molecule. This implies that a conformational reordering of this portion of eIF5 is likely to occur upon formation of a competent complex for GTP hydrolysis, following the appropriate activation signal. Interestingly, the N-terminal subdomain of eIF5 reveals an α/β fold structurally similar to both the archaeal orthologue of the β subunit of eIF2 and, unexpectedly, to eIF1. These results reveal a novel protein fold common to several factors involved in related steps of translation initiation. The implications of these observations are discussed in terms of the mechanism of translation initiation.

The initiation of protein synthesis in eukaryotic cells is a tightly regulated process entailing an intricate network of reversible protein−protein and protein−RNA interactions, as well as multiple phosphorylation events. It culminates with the assembly of a translation-competent 80S ribosome containing, in the P (peptidyl) site, the initiator methionyl-tRNA (Met-$tRNA_i^{Met}$) base paired with the AUG start codon of mRNA (*1*, *2*). Several proteins, termed eukaryotic initiation factors (eIFs),[1] are required for the correct execution and control of the translation initiation process (*1*, *3*). A key player in this process is the eIF2, a guanine nucleotide-binding protein, which, in its active GTP-bound state, recruits the Met-$tRNA_i^{Met}$ to the 40S ribosomal subunit. Upon identification of the initiating AUG codon of an mRNA, the GTP molecule bound to eIF2 is hydrolyzed to GDP in an irreversible reaction that requires eIF5, a GTPase-activating protein (GAP) (*4*, *5*), leading to the release of an inactive GDP−eIF2 complex from the ribosome. The reactivation of eIF2 for a successive round of translation initiation is accelerated by eIF2B, a guanine exchange factor (GEF), that catalyses the replacement of GDP for GTP (*1*, *3*, *6*).

Despite recent advances (*1*, *2*, *7*−*11*), the molecular events happening at the AUG codon recognition are still poorly understood. Recent data suggest that the release of P_i from eIF2·GDP, rather than the hydrolysis in itself, is the step that is controlled by start-codon recognition (*11*). Proper execution of this step is essential, because initiation of translation at incorrect codons would have devastating consequences for the cell by leading to the synthesis of

[†] This work was supported by a grant from The Wellcome Trust to M.R.C. and C.G.P. (068729).

[‡] Structures have been deposited in the Protein Data Bank (accession code 2G2K).

[*] To whom correspondence should be addressed. E-mail: sasi.conte@kcl.ac.uk. Telephone: +44-(0)207-8486194. Fax: +44-(0)207-8486435.

[§] University of Portsmouth.

[⊗] King's College London.

[||] Present address: Randall Division of Cell and Molecular Biophysics, King's College London, Guy's Campus, London SE1 1UL, United Kingdom.

[⊥] Biomedical NMR Centre, National Institute for Medical Research.

[#] Division of Protein Structure, National Institute for Medical Research.

[¶] The Walter and Eliza Hall Institute of Medical Research.

[£] University of Dundee.

[∞] University of British Columbia.

[▽] Present address: Department of Biochemistry and Molecular Biology, University of British Columbia, Life Sciences Centre, 2350 Health Sciences Mall, Vancouver, V6T 1Z3, Canada.

[1] Abbreviations: eIFs, eukaryotic initiation factors; aIF2, archaeal initiation factor 2; MFC, multifactor complex; GAP, GTPase activator protein; NMR, nuclear magnetic resonance; NOE, nuclear Overhauser effect; rmsd, root-mean-square deviation.

10.1021/bi052387u CCC: $33.50
Published on Web 03/18/2006

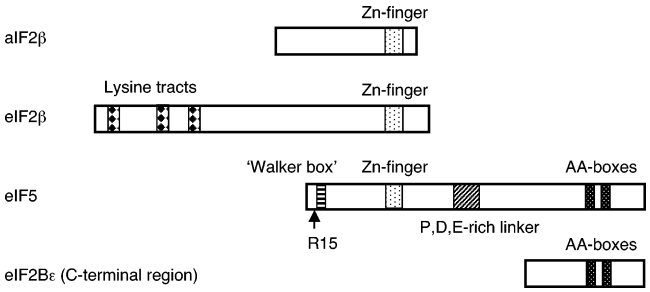

FIGURE 1: Structural and functional motifs of human eIF5 and its comparison with aIF2β, eIF2β, and the C-terminal region of the ϵ subunit of eIF2B. The region encompassing residues 194−394 of eIF5 shows high sequence homology with the region 523−712 of eIF2Bϵ, whereas the fragment spanning amino acids 33−125 of eIF5 has similarity at the level of the primary sequence with the region 217−307 of eIF2β. All of the numbering refers to human proteins.

miscoded proteins. Mutations in the genes encoding for factors eIF1, eIF2, and eIF5 result in the ability to initiate translation at UUG codons, indicating their involvement in start-site selection (*12*−*14*).

In the case of eIF5, the critical point mutation is located in the N-terminal region of the protein, which has been shown to contain the GAP function. The primary catalytic residue was identified as arginine 15 in the human protein (*4*, *5*) (Figure 1). Similar to the catalytic arginine of other arginine finger-type GAPs, Arg15 in eIF5 is flanked by hydrophobic (aromatic) residues (*4*, *15*). Two conserved lysine residues (K33 and K55) also appear to be required for GAP function (*5*). Adjacent to these lies an imperfect version of the Walker A box motif found in nucleotide-binding proteins. This is a highly conserved feature of eIF5 across species, but its function is presently unknown. Its possible involvement in interacting with GTP or GDP has been extensively investigated using a variety of methods, although no direct nucleotide binding was detected (*4*). The N-terminal half of eIF5 also contains a putative C_2-C_2 zinc finger (Figure 1), and some evidence has been presented that eIF5 binds nucleic acids in a zinc-dependent manner (*16*). Interestingly, the N-terminal region of eIF5 shares high sequence homology with a C-terminal portion of the β subunit of eIF2 (Figure 1); in the latter case, the zinc fingerlike domain has been shown to be important for the fidelity of AUG codon selection (*17*), suggesting that nucleic acid binding by this motif may have a possible role in start-site recognition or in the functional consequences of this recognition step that lead to GTP hydrolysis and eIF2 dissociation from the ribosomal complex. Alternatively, it is conceivable that the zinc finger domain of eIF5 is involved in the interaction with the homologous region of eIF2β (heterodimerization), bearing in mind the role of zinc finger domains in the homodimerization of CK2 subunits (*18*).

In addition to its GAP function, eIF5 also performs a different but equally important function in the translation initiation process. Studies in yeasts have shown that the C-terminal domain of eIF5 can interact with other components of the translation initiation apparatus, including eIF2, eIF1, eIF4G (a scaffold protein), and eIF3, a multisubunit factor responsible for promoting the interaction between the 40S subunit and the mRNA (*8*, *19*−*22*). Thus, a second function of eIF5 is in the assembly of a multifactor complex (MFC) leading to 48S initiation complex formation. The C-terminal portion of eIF5 shows sequence and perhaps structural similarities with the extreme C-terminal part of the catalytic subunit of eIF2B (eIF2Bϵ) in the region that binds their common substrate, eIF2, through the basic regions in the N-terminal part of eIF2β (*23*) (Figure 1). This interaction appears to be mediated by two AA boxes (rich in aromatic and acidic residues) conserved in eIF5, eIF2Bϵ, and also eIF4G (Figure 1). Finally, the central part of eIF5 (residues 175−210) abounds in prolines and acidic residues and may act as a disordered linker between the N-terminal GAP and C-terminal factor-interaction domains of eIF5.

eIF1, a small protein of only 12 kDa, is also a component of the MFC. Studies in yeast have shown that eIF1 associates with eIF3, eIF5 (via the C-terminal domain), and the ternary complex of eIF2·GTP·Met-tRNA$_i^{Met}$ (*19*, *20*, *23*−*26*). In mammals, eIF1 appears to enable 48S complexes to reject incorrect matches with the AUG codon (*27*) and association of eIF1 with eIF4G enhances the accuracy of scanning (*28*). It has been proposed that eIF1 functions to restrain the GAP activity of eIF5 (*7*, *9*, *10*); indeed, overexpression of eIF1 in yeast suppresses the otherwise high GAP activity of the eIF5(G31R) mutant (*9*), perhaps via a direct eIF1/eIF5 interaction. However, the most recent data (*11*) suggest that eIF1 impairs the release of P_i from eIF2·GDP rather that the hydrolytic step and that codon recognition may promote the dissociation of eIF1 from the 40S ribosomal complex.

In this paper, we report the solution structure of an N-terminal fragment of human eIF5 that reveals two subdomains reminiscent of nucleic-acid-binding motifs. Interaction studies with RNA though did not prove conclusive. The analysis of the GAP domain also appears to suggest that a conformational rearrangement may occur upon formation of a functioning complex capable of catalyzing GTP hydrolysis, although direct evidence for this is thus far lacking. Surprisingly, the N-terminal subdomain of eIF5 displays structural similarities to eIF1 despite no homology at the primary sequence level. This reveals a α/β sandwich fold that constitutes another common motif among translation initiation factors.

EXPERIMENTAL PROCEDURES

Plasmid Construction and Protein Expression. eIF5(1−170) was subcloned into a modified pET28a vector that adds a short N-terminal His tag as previously described (*29*, *30*). The protein was expressed in a BL21(DE3) pLysS *Escherichia coli* strain grown on minimal media enriched with 0.7 g L^{-1} ^{15}N-ammonium chloride and 2 g L^{-1} ^{13}C glucose plus 100 μM zinc chloride. Cells were grown at 37 °C until an OD_{600} of 0.3, then placed at 16 °C, and induced with 1 mM isopropyl-β-D-thiogalactopyranoside (IPTG) at an OD_{600} of 0.6. Cells were harvested 16 h after induction, resuspended in 20 mM Tris-HCl, 300 mM NaCl, and 10 mM imidazole at pH 8, and lysed by sonication. After centrifugation, the soluble fraction was purified by affinity chromatography on a Ni−NTA resin (Qiagen) using the protocol of the manufacturer. The eluted protein was dialyzed in 20 mM Tris-HCl, 100 mM KCl, and 2 mM dithiothreitol (DTT) at pH 7.25 and loaded on a 5 mL Hi-Trap Heparin column (Amersham Pharmacia Biotech). The protein was eluted with a linear 0−2.0 M KCl gradient in buffer A [50 mM Tris-HCl and 10% (v/v) glycerol at pH 7.25] and dialyzed in 20 mM sodium acetate and 2 mM DTT at pH 6.

Table 1: Summary of Structural Statistics for eIF5(1−170)

NMR restraints	eIF5(1−170)	
total distance restraints (interresidue)		
short−medium range (residue i to $i + j$, $j = 1-4$)	481	
long range (residue i to $i + j$, $j > 4$)	200	
hydrogen bond	42	
total dihedral angle restraints	204	
ϕ	102	
ψ	102	
restraints violations		
distance restraint violation > 0.2 Å	none	
dihedral restraint violation > 5°	none	
average rmsd (Å) among the 18 refined structures		
residues	**21−86**	**98−142**
backbone of structured regions[a]	0.66	0.92
heavy atoms of structured regions	1.45	1.69
backbone of all residues	1.017	1.38
heavy atoms of all residues	1.812	2.33
Ramachandran statistics of 18 structures		
percentage of residues in		
most favored regions	77	
additional allowed regions	16	
generously allowed regions	4.4	
disallowed regions	2.5	

[a] Residues selected on the basis of ^{15}N backbone dynamics. N-Terminal subdomain, 21−25, 33−45, and 50−86; C-terminal subdomain, 99−129 and 138−142.

NMR Spectroscopy. For NMR studies, pure eIF5(1−170) was concentrated to 0.6 mM in 700 or 300 μL. NMR spectra were recorded at 298 K on Varian Inova spectrometers operating at 14.1 and 18.8 T and on a Bruker Avance spectrometer at 14.1 T equipped with a triple resonance cryoprobe. The ^{1}H, ^{15}N, and ^{13}C resonance assignments for eIF5(1−170) is reported elsewhere (*J. Biomol. NMR*, manuscript submitted). NMRPipe/NMRDraw (*31*) was employed to process all spectra, which were then analyzed using XEASY (*32*). For structural calculation, nuclear Overhauser effect (NOE) distance restrains were obtained from ^{15}N- and ^{13}C-edited NOE spectrometry (NOESY)−heteronuclear single-quantum coherence (HSQC) experiments (*33*); backbone ϕ and ψ dihedral angles were obtained using TALOS software (*34*). Hydrogen-bonded amide protons were detected by analyzing a series of ^{1}H-^{15}N HSQC experiments up to 10 h after the proteins were buffer-exchanged in D_2O. T1, T2, and {^{1}H}-^{15}N NOE experiments were recorded using the pulse sequences adopted from standard schemes (*35*).

Structure Calculation. The solution structure of eIF5(1−170) was calculated using a combined torsion angle and Cartesian coordinates dynamics protocol executed in XPLOR (*36*). The structures were calculated from random starting coordinates on the basis of 681 NOE distance restraints, including 481 short-range (residue i to residue $i + j$, where $1 < j \leq 4$) and 200 long-range connectivities (residue i to residue $i + j$, where $j > 4$), 204 dihedral angle restraints (102 ϕ and 102 ψ angles), and 42 hydrogen-bond distance restraints. Notably, for large portions of the molecule (residues 2−21, 145−170, and the central part of helix α4), few short-range and no long-range NOE restraints could be detected.

The structures were analyzed using MolMol (*37*) and PROCHECK-NMR (*38*). Structures were displayed using MolMol and PyMOL (www.pymol.org). The final family comprised the 18 structures of the lowest total energy; structure statistics are shown in Table 1.

RESULTS

Tertiary Structure of the N-Terminal Region of eIF5. The protein used for structural studies included the entire region encompassing residues 1−170 from human eIF5, termed eIF5(1−170). In solution, eIF5(1−170) is monomeric and folds into two distinct subdomains connected by a long central helix (helix 4) spanning residues 82−97 (Figure 2). The first 6−7 amino acids of this helix form stable hydrophobic interactions with the most N-terminal subdomain that consists of four antiparallel β strands and three additional α helices exhibiting a α1β1β2α2α3β3β4α4 topology. The β sheet is closely packed on one side against helices α2, α3, and α4. Conversely, the first 20 residue stretch, which includes the helix α1, is not well-defined with respect to the rest of the molecule; no long-range NOE contacts could be unambiguously assigned, and its proposed intrinsic mobility is in agreement with backbone relaxation analysis and previous structural studies of the homologous β subunit of the archaeal initiation factor 2 (see below). The second subdomain contains a zinc finger motif, is composed of three β strands, generating a β5−β6−β7 antiparallel topology, and flanked on one side by helix α5. Zinc is coordinated by four highly conserved cysteines at positions 99, 102, 122, and 125 and is essential for the structural stability not only of this domain but also of the entire eIF5(1−170) fragment. The presence of zinc was confirmed by atomic absorption spectroscopy (data not shown). An apolar patch of the β sheet participates in a network of hydrophobic contacts with α5 and the C-terminal part of α4. The loop connecting strand β7 and helix α5 displays intrinsic flexibility in the nano−picosecond time scale, as well as the most C-terminal region spanning residues 146−170.

Because both subdomains interact extensively with residues at opposite ends of helix α4, they do not tumble fully independently from each other in solution; however, no unambiguous contacts between the two distinct portions of the molecule could be detected in the present experimental conditions. To further investigate the relative spatial orientation of the two subdomains, we attempted to obtain residual dipolar couplings of the NH vectors. Nonetheless, all of the liquid crystalline media employed, namely, alkyl-poly(ethylene glycol) (*39*), Pf1 phage (*40*), and compressed polyacrylamide gels (*41*, *42*), failed to produce any usable measurement because of unfolding, aggregation, and/or precipitation of the protein sample.

These data taken together indicate that, while the two subdomains of eIF5(1−170) are not completely mobile with respect to each other, a fixed orientation in solution could not be unambiguously found in our investigations. Therefore, each subdomain was superposed separately to calculate the root-mean-square deviation (rmsd). A final family of 18 superimposed structures for eIF5(19−87) and eIF5(94−145) is shown in Figure 2. The overall rmsd between the family and the mean coordinate position is 0.66 and 0.92 Å for backbone atoms in secondary-structured regions, respectively. The quality of the data reflects the challenges encountered in the structural analysis, because of instability of the sample compounded with aggregation and severe spectral overlap especially in the aromatic region. The structure calculation statistics are given in Table 1. The double-domain structure

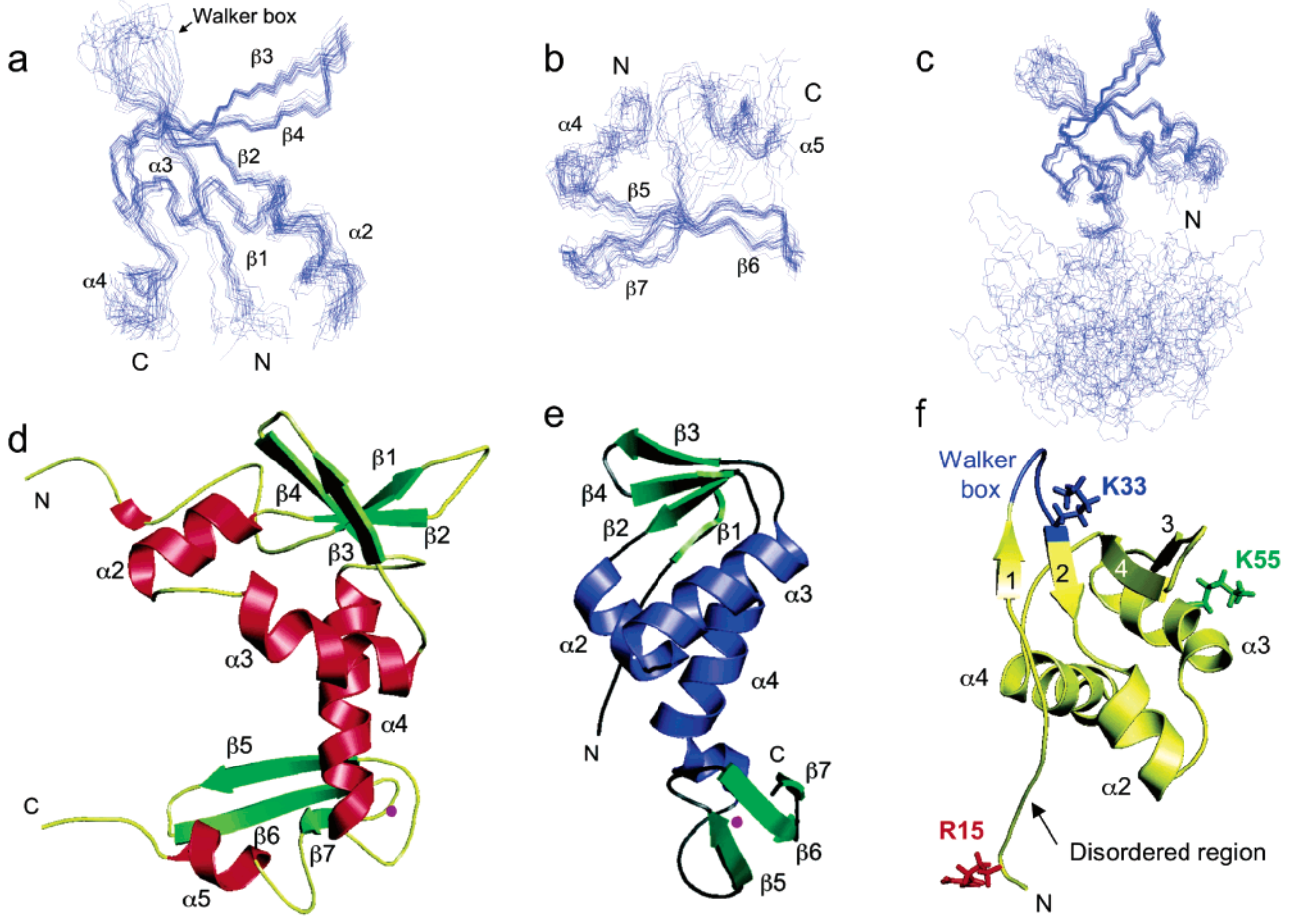

FIGURE 2: Structural analysis of eIF5. (a and b) Superimposition of the backbone traces for the 18 lowest energy structures for (a) the N-terminal subdomain (residues 19−89) and (b) C-terminal subdomain (94−145). The N and C termini and the secondary-structure elements are indicated. (c) Relative orientation of the two subdomains with respect to each other in the 18 lowest energy structures superposed on the N-terminal subdomain; whereas they are not fully mobile with respect to each other, long-range contacts could not be unambiguously detected in this study. (d) Diagram of eIF5(1−170) showing secondary-structure elements and N- and C-terminal flexible regions. The structure chosen corresponds to the lowest energy structure. (e) Comparison with aIF2β from *M. thermoautrophicum* (*43*). (f) N-Terminal subdomain of eIF5 with residues important for the GAP function. The imperfect Walker A box motif is highlighted in blue. The orientation is similar to that in a.

shown in Figure 2d represents the lowest energy structure obtained from the calculation.

The structure of eIF5(1−170) closely resembles the structure of the β subunit of archaeal initiation factor 2 (aIF2β) from *Methanococcus jannaschii* and *Methanobacterium thermoautotrophicum* (*43*, *44*) (Figure 2). This is not surprising because of the high sequence conservation between the N-terminal region of eIF5 and aIF2β. The main structural difference lies in the zinc finger domain, with eIF5 possessing the additional C-terminal α helix (α5). In contrast to aIF2β, in which this domain is capable of folding independently from the N-terminal domain (*44*), protein fragments expressing the isolated zinc finger domain from eIF5 failed to produce folded material (data not shown). A possible explanation resides in the presence in eIF5 of α5 that is stabilized by the apolar interactions with α4.

A partially unfolded N-terminal region is found in eIF5; backbone ^{1}H, ^{15}N, and ^{13}C assignments together with characteristic NOE patterns provide a strong indication of the propensity for a localized structure in these areas (*45*), but the lack of long-range NOE with residues preceding Ile21 coupled with relaxation analysis of the protein backbone (data not shown) supports the conclusion that this region is largely disordered. Several short−medium range NOE contacts were observable for residues 6−9 and 13−16, and for the former region, backbone chemical-shift values show evidence of the beginnings of the helical structure (termed α1 by analogy to the N-terminal region of eIF2β). These localized structures appear to involve hydrophobic side chains; Phe13, Tyr14, and Tyr16 in particular seem to form a cluster of aromatic residues, but the precise nature of the ring−ring interactions could not be determined because of spectral overlap. Overall, the relaxation analysis for the residues 5−19 indicates a conformational equilibrium between two or more partially populated states, with a significant population adopting a helical structure around residues 6−9. A similar result was also found for the N-terminal regions of both known aIF2β structures, despite lower sequence similarity with eIF5 in this region. Intriguingly, in the case of the eIF5 family of proteins, the N-terminal fragment is unique because it contains the primary arginine (Arg15) shown to be essential for the GAP function (see below). Equally, the N-terminal conserved region of archaeal aIF2β (corresponding to a central fragment of the eukaryotic eIF2β) that is not present in eIF5 is responsible for the stable interaction with eIF2γ (*46*). The eIF5/eIF2γ interaction is likely to occur transiently at the appropriate stage of the initiation/start-codon recognition process.

GAP Domain of eIF5. GAPs for the Rho and Ras family of small GTPases function by contributing a "primary" arginyl residue (termed the "arginine finger") to the active site of the GTP-binding protein, which by itself does not possess all of the catalytic groups required for GTP hydrolysis (*15*, *47*). These molecules all share a common architecture and all appear to function by inserting the "arginine finger" within reach of the G protein-bound GTP. The N-terminal region of eIF5 has been demonstrated to act as a GAP, whereby a invariant arginyl residue (Arg15 in mammalian eIF5) is required for the ability of eIF5 to promote the hydrolysis of GTP bound to eIF2 (*4*, *5*). This reaction appears to be a key element for the control of stringent selection of the AUG start codon during translation initiation (*12*), and the available data strongly support an arginine fingerlike role for Arg15 of eIF5 (*4*, *5*). The structure of eIF5 presented here reveals that the presumed catalytic Arg15 is, in fact, located within the disordered N-terminal region (Figure 2f). Thus, although the stereochemical basis of the transition-state stabilization by this residue may be quite similar to that observed in other related systems (RhoGAP/RasGAP structures) (*15*, *48*), the underlying pattern of protein−protein interactions must be quite different and is likely to entail a structural reordering of the partially disordered N-terminal arm upon formation of a GTP hydrolysis competent complex with eIF2γ. In such a complex, Arg15 could in fact relocate to the GTPase active site where it may act in an arginine fingerlike mechanism, as suggested by earlier reports (*4*, *5*). Alternatively, the invariant arginine 15 may play a role in stabilizing eIF5 binding through interactions with some other component of the initiation complex. Other interpretations are, of course, possible, and further investigations are needed to elucidate such a mechanism.

Most GAPs are specific for a member or subfamilies of GTP-binding proteins; members of different GAP subfamilies appear dissimilar at the level of the primary sequence, but in many cases, short conserved sequence motifs around the invariant arginine finger can be identified (*15*). Consistently, the invariant Arg15 in eIF5 is flanked by aromatic residues in the sequence FYRY, as seen for other arginine finger GAPs, and it is most closely related to that found in RhoGAPs (ϕYRϕ, where ϕ are hydrophobic residues) (*15*). The hydrophobic residues in RasGAP, RhoGAP, and related proteins pack into the core of the helical GAP domain and stabilize the arginine finger loop conformation (*15*, *47*). It is therefore possible that these residues in eIF5 play a similar role as part of a series of structural rearrangements that precede the introduction of Arg15 into the GTP-binding site during GTP hydrolysis.

Rho- and RasGAPs also contain a "secondary" positively charged residue (Arg or Lys), which has been shown to stabilize the finger loop (*15*, *47*). By analogy with other GAPs, the conserved lysines 33 and 55 in eIF5 have been proposed to participate in the GAP function, possibly acting as a structural equivalent to the secondary stabilizing Lys or Arg (*5*). The structure of eIF5 shows that these lysines are located in the N-terminal subdomain: K33 is at the beginning of strand β2, and K55 resides in the center of the helix α3 (Figure 2f). The now available structural information thus suggests that K55 is less likely to play this role, because it is located on the opposite side of the domain from the N-terminal arm. Although at this stage it is not possible to rule out any major structural reorganization within the core of the N-terminal subdomain of eIF5 upon codon recognition, K33 appears to be spatially positioned in a region of the molecule that may indeed be able to establish stabilizing interactions with the primary arginine in the eIF5−eIF2 GTP complex.

Interestingly, K33 is also contained within an imperfect Walker A box motif, which is a highly conserved region in eIF5 (but not present in eIF2β) and forms a loop between β strands 1 and 2. The importance of this motif for the GAP function is reinforced by the observation that the yeast SUI5 suppressor gene that can initiate translation in the absence of the AUG initiation codon is characterized by a single mutation Gly31 → Arg mutation (*12*). This residue corresponds to Gly31 in mammalian eIF5, and the structure presented here shows that substitution to arginine is likely to affect the conformation of this loop. While this variant Walker A motif has been shown not to bind GTP or GDP by itself and its role at present is obscure, it is intriguing to speculate that this region may function as a surrogate P-looplike structure in the right context at some stage in the initiation process.

eIF5 Is Structurally Related to eIF1 and Several Nucleic-Acid-Binding Proteins. According to a search of the protein structure matching server at EMBL-EBI (http://ebi.ac.uk/msd-srv/ssm) (*49*), the N-terminal subdomain of eIF5 (residues 19−90) is a close structural homologue of the scorpion toxin osk1 (*50*) ($Q \geq 0.31$; rmsd $\sim$ 2.21 Å over 53% of Cα), C-terminal domain of *E. coli* arginine repressor in complex with L-arginine (*51*) ($Q \geq 0.29$; rmsd $\sim$ 3.07 Å over 80% of Cα), KH1 from the fragile X-protein FMR1 (*52*) ($Q \geq 0.26$; rmsd $\sim$ 2.60 Å over 66% of Cα), and human translation factor eIF1 (*53*) ($Q \geq 0.24$; rmsd $\sim$ 2.23 Å over 85% of Cα). A number of these proteins have been shown to be involved in interactions with nucleic acids. Several proteins structurally related to the zinc finger subdomain (residues 97−143) were also identified: transcription elongation factor SII (*54*) ($Q \geq 0.31$; rmsd $\sim$ 1.89 Å over 72% of Cα), ribosomal protein L36 (*55*) ($Q \geq 0.30$; rmsd $\sim$ 1.70 Å over 59% of Cα), and the N-terminal domain of the transcription elongation factor TFIIB (*56*) ($Q \geq 0.23$; rmsd $\sim$ 2.85 Å over 72% of Cα). These data may be consistent with a role of eIF5 in nucleic acid recognition. Indeed, the zinc finger domain of eIF5 has been reported to bind single-stranded DNA and poly(U) RNA (*16*). Our preliminary investigations, however, did not prove conclusive of RNA-binding activity of eIF5 (data not shown), and further experiments are in progress.

As discussed previously, both eIF5 subdomains appear to be structurally similar to the corresponding regions found in archaeal aIF2β, in particular to the *M. jannaschii* protein (*44*) ($Q \geq 0.29$; rmsd $\sim$ 3.3 Å over 72% of Cα, and $Q \geq 0.36$; rmsd $\sim$ 2.00 Å over 68% of Cα, respectively); interestingly, mutations in the zinc finger region of eIF2β result in translation initiation at the UUG codon, highlighting its importance in stringent start-codon recognition (*17*). A specific role of the zinc finger domain of eIF5 has yet to be demonstrated.

The structure similarity between eIF5 and eIF1 is both intriguing and surprising; no sequence homology is detectable between the two proteins, but both factors play a fundamental role in AUG start-code selection. Figure 3 shows that most

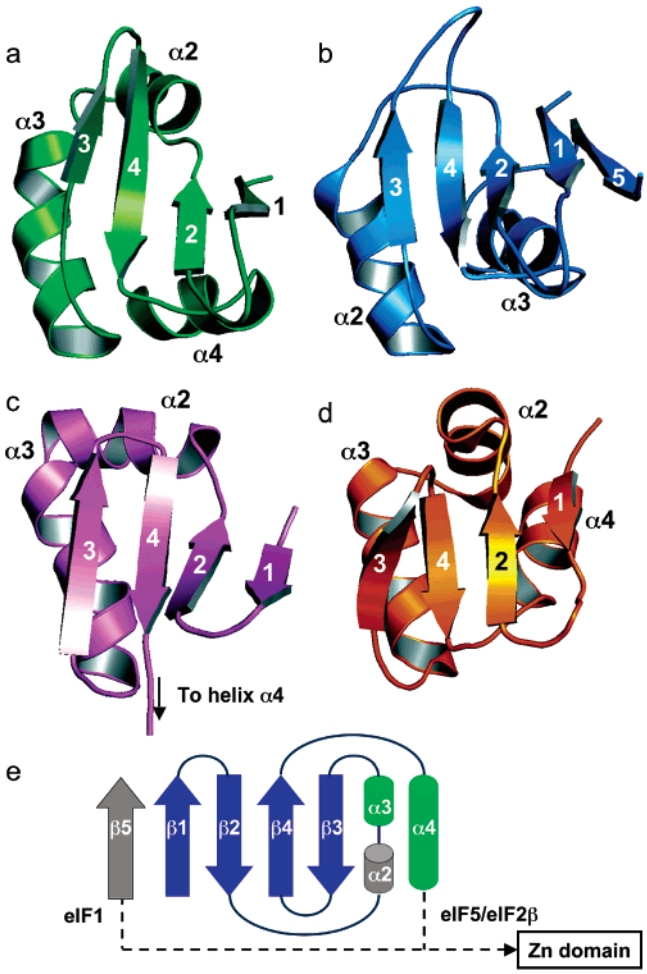

FIGURE 3: Structural comparison of the N-terminal domain of (a) eIF5 with (b) eIF1 (*53*) and the N-terminal domain of aIF2β (c) from *M. jannaschii* (*44*) and (d) from *M. thermoautrophicum* (*43*). Notably, the pdb file of *M. jannaschii* aIF2β did not contain helix α4. The topology of the common eIF125 fold is shown in e. Secondary elements in gray correspond to variations within the core fold. Furthermore, eIF5 and aIF2β have a longer helix α4 than the corresponding helix α3 in eIF1. Interestingly, all three factors contain a disordered N-terminal arm (not shown).

of the N-terminal subunit of eIF5 superposes well to the structure of eIF1, with the exception of helix α2, which is not included in the structure similarity. eIF1 also contains an element (strand β5) without a structural counterpart in eIF5. When these results are taken together, they show that eIF5, eIF2β, and eIF1 possess a common fold, characterized by a central four-stranded antiparallel β sheet with β1β2β4β3 topology, flanked on one side by two helices (α3 and α4 in eIF5/eIF2β and α2 and α3 in eIF1) (Figure 3). Extra secondary-structure elements can be found in addition to the core domain, in particular α2 in eIF5 and eIF2β and β5 in eIF1. Thus, we suggest that this α/β domain, termed the eIF125 fold, is another common fold found among translation initiation factors, in addition to RRM-, HEAT-, and OB-type domains (*3*, *6*). Furthermore, the N-terminal subdomain of eIF5 and eIF2β could be structurally related to the 4-stranded winged helix−turn−helix (wHTH) domains, including the prokaryotic *Crp* family and the eukaryotic HSF family (heat-shock transcription factors) (*57*), possibly suggesting a common wHTH evolutionary ancestor for the eIF125 domain. The comparison of the electrostatic surface potential for the eIF125 module of eIF1, eIF5, and eIF2β indicates a variety of surface properties for the three proteins, with eIF1 displaying the most marked basic and acidic character (data not shown).

Notably, the eIF125 fold appears only in archaeal and eukaryotic translation factors. Although a structural resemblance between eIF1 and the C-terminal domain of the prokaryotic initiation factor 3 (IF3) was previously reported (*3*), IF3 has, in fact, a different topology ($\beta\alpha\beta\alpha\beta\beta$ with a mixed β1β2β3β4 sheet) (*58*).

DISCUSSION

Eukaryotic initiation factor eIF5 is an essential component of the translation initiation machinery that commits the ribosomal complex to downstream events by activating the first irreversible step in the process, the hydrolysis of eIF2-bound GTP. Recently, parallel studies carried out in several laboratories have convincingly demonstrated that start-codon recognition is accompanied by structural rearrangements of the 43S ribosomal complex (*7*, *8*, *10*, *11*); nonetheless, the molecular details of how this is linked to GTP hydrolysis and the release of the factors still remain obscure. The structure of eIF5(1−170) presented here reveals that eIF5 is the only arginine-type GAP known thus far with the primary arginine located in a partially unfolded region, suggesting that a structural reordering of this fragment occurs in the interaction with eIF2γ during 40S ribosomal complex activation, perhaps in a manner similar to that observed for the disordered region of eIF4G following an eIF4E interaction (*59*). The C-terminal domain of eIF5 contains a highly conserved bipartite motif involved in simultaneous binding to the lysine box region of eIF2β; presumably, while this interaction represents the initial docking event, the N-terminal domain of eIF5 contacts the nucleotide-binding pocket of eIF2γ to catalyze the GTP hydrolysis, following the correct activation signal. This mechanism suggests a complex interplay between different domains and subunits of eIF2 and eIF5.

It is tempting to speculate that the required conformational reorganization of eIF5 for the timely activation of the GTP hydrolysis could be promoted by the interaction with other components within the ribosomal complex, including nucleic acids, although the current evidence does not argue strongly for an RNA-binding property of eIF5 (see above). Recent studies of the β2-chimerin have indeed portrayed the role of the domain−domain interaction in exerting control on GAP activity; only when lipid binding to β2-chimerin occurs, a large conformational change exposes its RacGAP domain, allowing it to bind to the GTP-binding protein (*60*).

The structure presented here shows that eIF5 is the first GAP, to our knowledge, to resemble nucleic-acid-binding proteins. However, in our opinion, the most remarkable finding is that the N-terminal subunit of eIF5 shows striking three-dimensional similarity to eIF2β and eIF1, with the latter unanticipated from primary sequence analysis. The reiterative use of common folds appears to be a frequent trait in translation initiation factors, and this α/β sandwich module, termed the eIF125 fold, joins the ranks of other conserved domains (OB, HEAT, and RRM). Interestingly, the eIF125 fold is not conserved in the prokaryotic translation initiation apparatus; however, the similarity among archaeal and eukaryotic factors points toward a common evolutionary ancestor.

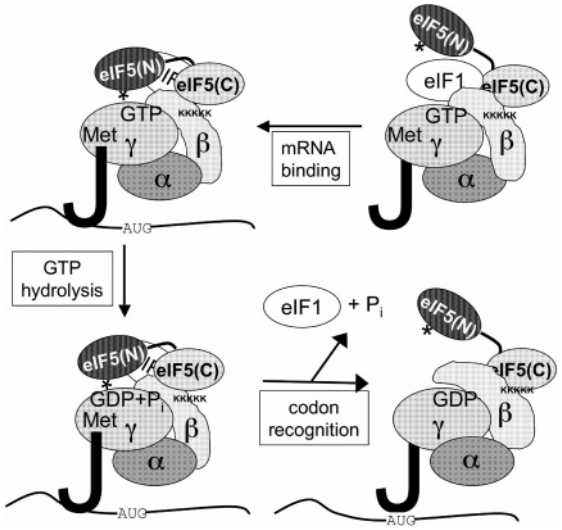

FIGURE 4: Possible mechanism for the roles of eIF1, eIF2, and eIF5 in translation initiation. The C-terminal domain of eIF5 [eIF5-(C)] interacts with lysine blocks (KKKKK) in eIF2β and with eIF1. Although no interaction between eIF5(N) and eIF2γ has yet been demonstrated, given that eIF5 is the GAP for this GTP-binding subunit of eIF2, such an interaction must presumably occur, although it may be too transient to detect easily. In this model, we speculate that binding of mRNA results in a conformational change that removes eIF1 from proximity to eIF2γ (which binds GTP), allowing the structurally similar N-terminal region of eIF5 [eIF5-(N) containing the catalytic arginine*] to move into place next to the GTP, resulting in GTP hydrolysis. After correct codon/anticodon pairing between Met-tRNA$_i$ and the start codon, a further rearrangement occurs, involving or resulting in a conformational change in eIF2β. This causes the release of eIF1 and P_i and allows eIF2β to move relative to eIF2$\alpha\gamma$. eIF2β consequently occupies (part of) the space formerly occupied by the structurally homologous N-terminal domain of eIF5 (see the text). Subsequent events are not depicted here.

The structure of the N-terminal half of eIF5 presented here and its structural similarities to eIF1 and eIF2β could help elucidate the molecular mechanisms that trigger the irreversible GTP hydrolysis upon AUG recognition. Given the tight functional links between these factors, it is alluring to hypothesise that their structural resemblance also has mechanistic significance. This leads us to propose a possible model for the concerted action of eIF1, eIF5, and eIF2β during start-codon recognition and GTP hydrolysis, depicted schematically in Figure 4. We anticipate that this exploratory model will provoke further discussion and experimental analysis.

In this speculative model, we propose that eIF1, bound to the C-terminal domain of eIF5, is positioned close to eIF2γ, thereby sterically impeding its interaction with the N-terminal GAP domain of eIF5 and therefore repressing GTP hydrolysis. This activity of eIF1 is thought to occur in the context of the MFC. It is important to point out that the existence of the MFC is based on data from yeasts, and it remains to be established whether an analogous complex also exists in mammals. Nonetheless, given the high degrees of similarity between the translation factors and between other aspects of translation in the two systems, we feel it is not unreasonable to suggest that translation initiation in mammals does also involve a similar type of complex. In the first conformational switch induced by mRNA binding (*11*), a conformational and/or electrostatic change in the local environment displaces eIF1, allowing the GAP domain of eIF5 to form a complex with eIF2γ that is competent for GTP hydrolysis. Finally, the second structural rearrangement following AUG codon recognition is accompanied by the release of P_i and eIF1 from the ribosomal complex (*11*). In our model, we propose a rearrangement within the eIF2 subunits (now in a binary complex with GDP), whereby the β subunit moves to the site just occupied by the GAP domain of eIF5 and previously by eIF1. This could weaken the affinity of eIF2 for the ribosome (or MFC), resulting in its release. The proposed mechanism could be guided kinetically, with the dwell time of the ribosome at a specific codon determining the likelihood that the conformational change leading to eIF2β movement and eIF1 release occurs.

The structural determination of isolated initiation factors or subunits is undoubtedly a valuable first step in elucidating the molecular mechanism of key stages of initiation of protein synthesis. A detailed understanding of the nature of the intricate interplay between the factors, to confirm, modify, or refute proposed mechanisms, awaits structural information of ribosomal complexes at a different stage of the initiation process.

ACKNOWLEDGMENT

We thank Dr. Marco Trifuoggi, University of Naples, Italy, for atomic absorption measurements and Drs. Edith Gomez and Graham Dunn for help at the early stages of the project.

REFERENCES

1. Dever, T. E. (2002) Gene-specific regulation by general translation factors, *Cell 108*, 545−556.
2. Kapp, L. D., and Lorsch, J. R. (2004) The molecular mechanics of eukaryotic translation, *Annu. Rev. Biochem. 73*, 657−704.
3. Sonenberg, N., and Dever, T. E. (2003) Eukaryotic translation initiation factors and regulators, *Curr. Opin. Struct. Biol. 13*, 56−63.
4. Paulin, F. E., Campbell, L. E., O'Brien, K., Loughlin, J., and Proud, C. G. (2001) Eukaryotic translation initiation factor 5 (eIF5) acts as a classical GTPase-activator protein, *Curr. Biol. 11*, 55−59.
5. Das, S., Ghosh, R., and Maitra, U. (2001) Eukaryotic translation initiation factor 5 functions as a GTPase-activating protein, *J. Biol. Chem. 276*, 6720−6726.
6. Boesen, T., Mohammad, S. S., Pavitt, G. D., and Andersen, G. R. (2004) Structure of the catalytic fragment of translation initiation factor 2B and identification of a critically important catalytic residue, *J. Biol. Chem. 279*, 10584−10592.
7. Maag, D., Fekete, C. A., Gryczynski, Z., and Lorsch, J. R. (2005) A conformational change in the eukaryotic translation preinitiation complex and release of eIF1 signal recognition of the start codon, *Mol. Cell 17*, 265−275.
8. Majumdar, R., and Maitra, U. (2005) Regulation of GTP hydrolysis prior to ribosomal AUG selection during eukaryotic translation initiation, *EMBO J. 24*, 3737−3746.
9. Valasek, L., Nielsen, K. H., Zhang, F., Fekete, C. A., and Hinnebusch, A. G. (2004) Interactions of eukaryotic translation initiation factor 3 (eIF3) subunit NIP1/c with eIF1 and eIF5 promote preinitiation complex assembly and regulate start codon selection, *Mol. Cell. Biol. 24*, 9437−9455.
10. Unbehaun, A., Borukhov, S. I., Hellen, C. U., and Pestova, T. V. (2004) Release of initiation factors from 48S complexes during ribosomal subunit joining and the link between establishment of codon−anticodon base-pairing and hydrolysis of eIF2-bound GTP, *Genes Dev. 18*, 3078−3093.
11. Algire, M. A., Maag, D., and Lorsch, J. R. (2005) P_i release from eIF2, not GTP hydrolysis, is the step controlled by start-site selection during eukaryotic translation initiation, *Mol. Cell 20*, 251−262.
12. Huang, H. K., Yoon, H., Hannig, E. M., and Donahue, T. F. (1997) GTP hydrolysis controls stringent selection of the AUG start codon during translation initiation in *Saccharomyces cerevisiae*, *Genes Dev. 11*, 2396−2413.

13. Yoon, H. J., and Donahue, T. F. (1992) The suil suppressor locus in *Saccharomyces cerevisiae* encodes a translation factor that functions during tRNA(iMet) recognition of the start codon, *Mol. Cell. Biol. 12*, 248−260.
14. Cui, Y., Dinman, J. D., Kinzy, T. G., and Peltz, S. W. (1998) The Mof2/Sui1 protein is a general monitor of translational accuracy, *Mol. Cell. Biol. 18*, 1506−1516.
15. Scheffzek, K., Ahmadian, M. R., and Wittinghofer, A. (1998) GTPase-activating proteins: Helping hands to complement an active site, *Trends Biochem. Sci. 23*, 257−262.
16. Ribera, I. L., Ruiz-Avila, L., and Puigdomenech, P. (1997) The eukaryotic translation initiation factor 5, eIF-5, a protein from *Zea mays*, containing a zinc-finger structure, binds nucleic acids in a zinc-dependent manner, *Biochem. Biophys. Res. Commun. 236*, 510−516.
17. Donahue, T. F., Cigan, A. M., Pabich, E. K., and Valavicius, B. C. (1988) Mutations at a Zn(II) finger motif in the yeast eIF-2β gene alter ribosomal start-site selection during the scanning process, *Cell 54*, 621−632.
18. Chantalat, L., Leroy, D., Filhol, O., Nueda, A., Benitez, M. J., Chambaz, E. M., Cochet, C., and Dideberg, O. (1999) Crystal structure of the human protein kinase CK2 regulatory subunit reveals its zinc finger-mediated dimerization, *EMBO J. 18*, 2930−2940.
19. Asano, K., Clayton, J., Shalev, A., and Hinnebusch, A. G. (2000) A multifactor complex of eukaryotic initiation factors, eIF1, eIF2, eIF3, eIF5, and initiator tRNA(Met) is an important translation initiation intermediate in vivo, *Genes Dev. 14*, 2534−2546.
20. Asano, K., Shalev, A., Phan, L., Nielsen, K., Clayton, J., Valasek, L., Donahue, T. F., and Hinnebusch, A. G. (2001) Multiple roles for the C-terminal domain of eIF5 in translation initiation complex assembly and GTPase activation, *EMBO J. 20*, 2326−2337.
21. Bandyopadhyay, A., and Maitra, U. (1999) Cloning and characterization of the p42 subunit of mammalian translation initiation factor 3 (eIF3): Demonstration that eIF3 interacts with eIF5 in mammalian cells, *Nucleic Acids Res. 27*, 1331−1337.
22. Yamamoto, Y., Singh, C. R., Marintchev, A., Hall, N. S., Hannig, E. M., Wagner, G., and Asano, K. (2005) The eukaryotic initiation factor (eIF) 5 HEAT domain mediates multifactor assembly and scanning with distinct interfaces to eIF1, eIF2, eIF3, and eIF4G, *Proc. Natl. Acad. Sci. U.S.A.*
23. Asano, K., Krishnamoorthy, T., Phan, L., Pavitt, G. D., and Hinnebusch, A. G. (1999) Conserved bipartite motifs in yeast eIF5 and eIF2Bϵ, GTPase-activating and GDP−GTP exchange factors in translation initiation, mediate binding to their common substrate eIF2, *EMBO J. 18*, 1673−1688.
24. Valasek, L., Mathew, A. A., Shin, B. S., Nielsen, K. H., Szamecz, B., and Hinnebusch, A. G. (2003) The yeast eIF3 subunits TIF32/a, NIP1/c, and eIF5 make critical connections with the 40S ribosome in vivo, *Genes Dev. 17*, 786−799.
25. Valasek, L., Nielsen, K. H., and Hinnebusch, A. G. (2002) Direct eIF2−eIF3 contact in the multifactor complex is important for translation initiation in vivo, *EMBO J. 21*, 5886−5898.
26. Phan, L., Zhang, X., Asano, K., Anderson, J., Vornlocher, H. P., Greenberg, J. R., Qin, J., and Hinnebusch, A. G. (1998) Identification of a translation initiation factor 3 (eIF3) core complex, conserved in yeast and mammals, that interacts with eIF5, *Mol. Cell. Biol. 18*, 4935−4946.
27. Pestova, T. V., and Kolupaeva, V. G. (2002) The roles of individual eukaryotic translation initiation factors in ribosomal scanning and initiation codon selection, *Genes Dev. 16*, 2906−2922.
28. He, H., von der Haar, T., Singh, C. R., Ii, M., Li, B., Hinnebusch, A. G., McCarthy, J. E., and Asano, K. (2003) The yeast eukaryotic initiation factor 4G (eIF4G) HEAT domain interacts with eIF1 and eIF5 and is involved in stringent AUG selection, *Mol. Cell. Biol. 23*, 5431−5445.
29. Alfano, C., Sanfelice, D., Babon, J., Kelly, G., Jacks, A., Curry, S., and Conte, M. R. (2004) Structural analysis of cooperative RNA binding by the La motif and central RRM domain of human La protein, *Nat. Struct. Mol. Biol. 11*, 323−329.
30. Alfano, C., Babon, J., Kelly, G., Curry, S., and Conte, M. R. (2003) Resonance assignment and secondary structure of an N-terminal fragment of the human La protein, *J. Biomol. NMR 27*, 93−94.
31. Delaglio, F., Grzesiek, S., Vuister, G. W., Zhu, G., Pfeifer, J., and Bax, A. (1995) NMRPipe: A multidimensional spectral processing system based on UNIX pipes, *J. Biomol. NMR 6*, 277−293.
32. Bartels, C., Xia, T., Billeter, M., Güntert, P., and Wüthrich, K. (1995) The program XEASY for computer supported NMR spectral-analysis of biological macromolecules, *J. Biomol. NMR 6*, 1−10.
33. Fesik, S. W., and Zuiderweg, E. R. P. (1988) Heteronuclear 3-dimensional NMR spectroscopy. A strategy for the simplification of homo-nuclear two-dimensional NMR spectra, *J. Magn. Reson. 78*, 588−593.
34. Cornilescu, G., Delaglio, F., and Bax, A. (1999) Protein backbone angle restraints from searching a database for chemical shift and sequence homology, *J. Biomol. NMR 13*, 289−302.
35. Kay, L. E., Torchia, D. A., and Bax, A. (1989) Backbone dynamics of proteins as studied by ^{15}N inverse detected heteronuclear NMR spectroscopy: Application to staphylococcal nuclease, *Biochemistry 28*, 8972−8979.
36. Brünger, A. T. (1993) Yale University, New Haven, CT.
37. Koradi, R., Billeter, M., and Wuthrich, K. (1996) MOLMOL: A program for display and analysis of macromolecular structures, *J. Mol. Graphics 14*, 51−55, 29−32.
38. Laskowski, R. A., Rullmannn, J. A., MacArthur, M. W., Kaptein, R., and Thornton, J. M. (1996) AQUA and PROCHECK-NMR: Programs for checking the quality of protein structures solved by NMR, *J. Biomol. NMR 8*, 477−486.
39. Rückert, M., and Otting, G. (2000) Alignment of biological macromolecules in novel non-ionic liquid crystalline media for NMR experiments, *J. Am. Chem. Soc. 122*, 7793−7797.
40. Hansen, M. R., Mueller, L., and Pardi, A. (1998) Tunable alignment of macromolecules by filamentous phage yields dipolar coupling interactions, *Nat. Struct. Biol. 5*, 1065−1074.
41. Ishii, Y., Markus, M. A., and Tycko, R. (2001) Controlling residual dipolar couplings in high-resolution NMR of proteins by strain induced alignment in a gel, *J. Biomol. NMR 21*, 141−151.
42. Sass, H. J., Musco, G., Stahl, S. J., Wingfield, P. T., and Grzesiek, S. (2000) Solution NMR of proteins within polyacrylamide gels: Diffusional properties and residual alignment by mechanical stress or embedding of oriented purple membranes, *J. Biomol. NMR 18*, 303−309.
43. Gutierrez, P., Osborne, M. J., Siddiqui, N., Trempe, J. F., Arrowsmith, C., and Gehring, K. (2004) Structure of the archaeal translation initiation factor aIF2β from *Methanobacterium thermoautotrophicum*: Implications for translation initiation, *Protein Sci. 13*, 659−667.
44. Cho, S., and Hoffman, D. W. (2002) Structure of the β subunit of translation initiation factor 2 from the archaeon *Methanococcus jannaschii*: A representative of the eIF2β/eIF5 family of proteins, *Biochemistry 41*, 5730−5742.
45. Yao, J., Chung, J., Eliezer, D., Wright, P. E., and Dyson, H. J. (2001) NMR structural and dynamic characterization of the acid-unfolded state of apomyoglobin provides insights into the early events in protein folding, *Biochemistry 40*, 3561−3571.
46. Thompson, G. M., Pacheco, E., Melo, E. O., and Castilho, B. A. (2000) Conserved sequences in the beta subunit of archaeal and eukaryal translation initiation factor 2 (eIF2), absent from eIF5, mediate interaction with eIF2γ, *Biochem. J. 347* (part 3), 703−709.
47. Gamblin, S. J., and Smerdon, S. J. (1998) GTPase-activating proteins and their complexes, *Curr. Opin. Struct. Biol. 8*, 195−201.
48. Rittinger, K., Taylor, W. R., Smerdon, S. J., and Gamblin, S. J. (1998) Support for shared ancestry of GAPs, *Nature 392*, 448−449.
49. Krissinel, E., and Henrick, K. (2004) Secondary-structure matching (SSM), a new tool for fast protein structure alignment in three dimensions, *Acta Crystallogr., Sect. D: Biol. Crystallogr. 60*, 2256−2268.
50. Jaravine, V. A., Nolde, D. E., Reibarkh, M. J., Korolkova, Y. V., Kozlov, S. A., Pluzhnikov, K. A., Grishin, E. V., and Arseniev, A. S. (1997) Three-dimensional structure of toxin OSK1 from *Orthochirus scrobiculosus* scorpion venom, *Biochemistry 36*, 1223−1232.
51. van Duyne, G. D., Ghosh, G., Maas, W. K., and Sigler, P. B. (1996) Structure of the oligomerization and L-arginine binding domain of the arginine repressor of *Escherichia coli*, *J. Mol. Biol. 256*, 377−391.
52. Musco, G., Kharrat, A., Stier, G., Fraternali, F., Gibson, T. J., Nilges, M., and Pastore, A. (1997) The solution structure of the first KH domain of FMR1, the protein responsible for the fragile X syndrome, *Nat. Struct. Biol. 4*, 712−716.

53. Fletcher, C. M., Pestova, T. V., Hellen, C. U., and Wagner, G. (1999) Structure and interactions of the translation initiation factor eIF1, *EMBO J. 18*, 2631−2637.
54. Qian, X., Gozani, S. N., Yoon, H., Jeon, C. J., Agarwal, K., and Weiss, M. A. (1993) Novel zinc finger motif in the basal transcriptional machinery: Three-dimensional NMR studies of the nucleic acid binding domain of transcriptional elongation factor TFIIS, *Biochemistry 32*, 9944−9959.
55. Hard, T., Rak, A., Allard, P., Kloo, L., and Garber, M. (2000) The solution structure of ribosomal protein L36 from *Thermus thermophilus* reveals a zinc-ribbon-like fold, *J. Mol. Biol. 296*, 169−180.
56. Zhu, W., Zeng, Q., Colangelo, C. M., Lewis, M., Summers, M. F., and Scott, R. A. (1996) The N-terminal domain of TFIIB from *Pyrococcus furiosus* forms a zinc ribbon, *Nat. Struct. Biol. 3*, 122−124.
57. Aravind, L., Anantharaman, V., Balaji, S., Babu, M. M., and Iyer, L. M. (2005) The many faces of the helix−turn−helix domain: Transcription regulation and beyond, *FEMS Microbiol. Rev. 29*, 231−262.
58. Biou, V., Shu, F., and Ramakrishnan, V. (1995) X-ray crystallography shows that translational initiation factor IF3 consists of two compact α/β domains linked by an α-helix, *EMBO J. 14*, 4056−4064.
59. Gross, J. D., Moerke, N. J., von der Haar, T., Lugovskoy, A. A., Sachs, A. B., McCarthy, J. E., and Wagner, G. (2003) Ribosome loading onto the mRNA cap is driven by conformational coupling between eIF4G and eIF4E, *Cell 115*, 739−750.
60. Canagarajah, B., Leskow, F. C., Ho, J. Y., Mischak, H., Saidi, L. F., Kazanietz, M. G., and Hurley, J. H. (2004) Structural mechanism for lipid activation of the Rac-specific GAP, β2-chimaerin, *Cell 119*, 407−418.

BI052387U